

Erratum

Disrupted flow sensing impairs hydrodynamic performance and increases the metabolic cost of swimming in the yellowtail kingfish, *Seriola lalandi*

Kazutaka Yanase, Neill A. Herbert and John C. Montgomery

10.1242/jeb.082107

There was an error published in *J. Exp. Biol.* **215**, 3944-3954.

On p.3947, the π in Eqn 3 was incorrectly displayed as a δ . The equation should have read:

$$A_f = \pi dw/4.$$

We apologise to the authors and readers for any inconvenience that this error may have caused.

RESEARCH ARTICLE

Disrupted flow sensing impairs hydrodynamic performance and increases the metabolic cost of swimming in the yellowtail kingfish, *Seriola lalandi*

Kazutaka Yanase*, Neill A. Herbert and John C. Montgomery

Leigh Marine Laboratory, University of Auckland, 160 Goat Island Road, Leigh 0985, New Zealand

*Author for correspondence at present address: Department of Energy and Process Engineering, Tampere University of Technology, Korkeakoulunkatu 6, FI-33101 Tampere, Finland (kazutaka.yanase@gmail.com)

SUMMARY

The yellowtail kingfish, *Seriola lalandi*, shows a distribution of anaerobic and aerobic (red and pink) muscle fibres along the trunk that is characteristic of active pelagic fishes. The athletic capacity of *S. lalandi* is also shown by its relative high standard metabolic rate and optimal (i.e. least cost) swimming speed. To test the hypothesis that lateral line afferent information contributes to efficient locomotion in an active pelagic species, the swimming performance of *S. lalandi* was evaluated after unilateral disruption of trunk superficial neuromasts (SNs). Unilaterally disrupting the SNs of the lateral line impaired both swimming performance and energetic efficiency. The critical swimming speed (U_{crit} ; mean \pm s.d., $N=12$) for unilaterally SN-disrupted fish was 2.11 ± 0.96 fork lengths (FL) s^{-1} , which was significantly slower than the 3.66 ± 0.19 FL s^{-1} U_{crit} of sham SN-disrupted fish. The oxygen consumption rate ($mg O_2 kg^{-1} min^{-1}$) of the unilaterally SN-disrupted fish in a speed range of 1.0 – 2.2 FL s^{-1} was significantly greater than that of the sham SN-disrupted fish. The least gross cost of transport (GCOT; $N=6$) for SN-disrupted fish was 0.18 ± 0.06 J $N^{-1} m^{-1}$, which was significantly greater than the 0.11 ± 0.03 J $N^{-1} m^{-1}$ GCOT for sham SN-disrupted fish. The factorial metabolic scope ($N=6$) of the unilaterally SN-disrupted fish (2.87 ± 0.78) was significantly less than that of sham controls (4.14 ± 0.37). These data show that an intact lateral line is important to the swimming performance and efficiency of carangiform swimmers, but the functional mechanism of this effect remains to be determined.

Key words: lateral line, superficial neuromast, standard metabolic rate, cost of transport, oxygen consumption, critical swimming speed, feedback motor control, kingfish, *Seriola lalandi*.

Received 5 April 2012; Accepted 22 July 2012

INTRODUCTION

In contrast to animals with aerial or terrestrial locomotion, aquatic locomotion in fishes is affected to a greater extent by forces, i.e. pressure drag and viscous drag, resulting in severe restrictions on forward speed and energetic performance due to the high density and viscosity of the aquatic medium (Schmidt-Nielsen, 1972; Daniel and Webb, 1987; Fish, 1994). These drags increase with increased swimming speed, and also increase as a result of thrust production through the movements of the trunk and the tail fin (Anderson et al., 2001). Given the metabolic benefits of a lowered cost of locomotion for a given swimming speed, and the complex interaction of boundary layers, drag and thrust production, it seems reasonable that active flow sensing by fish could play a part in improving the efficiency of locomotion. Active flow sensing by the lateral line has been shown to be important in allowing fish to seek out flow refuges generated by obstacles in the flow (Montgomery et al., 2003), and in allowing fish to modify their swimming and save energy in structured turbulent flows (Liao et al., 2003). However, a direct contribution of the lateral line to efficient swimming has not yet been shown for fish swimming under normal conditions.

Two potential roles for a contribution of lateral-line feedback to swimming efficiency have been proposed. Lighthill (Lighthill, 1993) suggested that the lateral-line sensors in the subcerebral canal system of the herring could provide an appropriate feedback signal for controlling yaw by oscillatory neck deflections so as to minimize the effective pressure difference and any associated cross-flow effects

over the head of the fish. It was proposed that swimming clupeid fishes may use this as an ‘active’ mechanism for reduction of hydrodynamic resistance. This theory was supported by analysis of the mechanics of the subcerebral perilymph canal, which crosses the head between the lateral lines of clupeid fishes (Denton and Gray, 1993), and an analysis of the head turning movements in herring and other fishes (Rowe et al., 1993). However, direct experimental evidence for a role of lateral-line feedback in this behaviour was not provided in those studies. A recent study by McHenry et al. (McHenry et al., 2010) in a different species of fish (golden shiner, *Notemigonus crysoleucas*) concluded from kinematic analysis that ‘flow sensing does not facilitate active drag reduction’, at least with respect to coordinating the motion of the head relative to detected flow signals. However, the golden shiner is not a particularly active species, and this study does not provide any direct measures of swimming efficiency relative to the manipulation of the lateral line.

The second suggested role for lateral-line feedback in the efficient control of swimming came from the detailed measurements of the thin layers of flowing water immediately adjacent to the surface of the swimming fish (i.e. the boundary layers), where influence of viscosity predominates (Anderson et al., 2001). This study observed inflected boundary layers that appeared to be stabilized during the later phases of the undulatory cycle, and suggested that these boundary layer profiles may provide evidence of a contribution of hydrodynamic sensing to the optimization of swimming performance. But, again, this suggestion remains to be directly tested.

The lateral line of fish is made up of two submodalities, canal neuromasts and superficial neuromasts (SNs). The canal neuromasts respond less to steady currents and low-frequency flows, and are better suited to encode higher frequency signals (Montgomery et al., 2001). The SNs, in contrast, have anatomically appropriate properties to sense steady currents and low-frequency flows immediately above the surface of the fish body (Coombs and Janssen, 1989; Coombs and Janssen, 1990; Kroese and Schellart, 1992; Montgomery et al., 1994). Therefore, SNs are the most likely submodality to contribute to motor control for sustained or prolonged level of swimming associated with boundary layer flows. Here we experimentally test the hypothesis that the SNs of the trunk lateral line contribute to swimming efficiency. The critical swimming speed, U_{crit} , and metabolic cost of locomotion were measured in an active pelagic species, the yellowtail kingfish, *Seriola lalandi* Valenciennes 1833. The premise that should be supported in the present study is that the yellowtail kingfish is an active pelagic species where active flow sensing for swimming efficiency is likely to be important. The muscle locomotor system in fishes contains two functionally independent components, designated red and white muscle due to their usual colour (Lindsey, 1978). Although the white muscle is faster, more powerful and capable of burst activity, which may be anaerobic, the red muscle is usually slow with low contractile power. The relative development of red and white muscle in different species may be correlated roughly with their mode of life (Videler, 1993; Ellerby and Altringham, 2001). Therefore, we conducted macroscopic examination of locomotor muscle of *S. lalandi*, by which the active athletic nature of this species was documented based on the relative mass proportion of the red muscle and cross-sectional profiles of muscle fibre types that were found. The constant rhythmic oscillatory tail motion that is usually found in prolonged swimming activity, such as migration, foraging, etc., is predominantly powered by aerobic metabolism (Hudson, 1973; Webb, 1975). Such an aerobically powered mode of swimming demonstrates a linear increase in oscillatory tail-beat frequency with increased swimming speed, resulting in an exponential increase in oxygen demand with increased swimming speed (Lowe et al., 1998; Lowe, 2001; Webber et al., 2001; Steinhausen et al., 2005). Measuring the rate at which oxygen is consumed during locomotion is therefore a direct and non-invasive way to determine the physiological cost of locomotion and is commonly undertaken in accordance with incremental velocity tests, which measure U_{crit} (Brett, 1964). These measurements were made for control fish, and fish with a unilateral ablation of the trunk SNs.

The control system for rhythmic animal locomotion, including fish swimming, is formed by sets of neurons in the central nervous system, the so-called central pattern generators (CPGs) (Tytell and Cohen, 2008). The CPGs exhibit certain properties of adaptation and robustness to the environmental changes by generating rhythmic neural output, where the feedback is not essential (Iwasaki and Zheng, 2006). The CPGs, however, receive sensory feedback capable of modulating their rhythmic activity in order to achieve adaptation to environmental changes (Iwasaki and Zheng, 2006). The simplest explanation of the mechanism of CPG activity may be given by the reciprocal inhibition oscillator (Brown, 1911) located in the spinal cord (Friesen, 1994). The CPG consists of two pools of interneurons mutually coupled with inhibitory synaptic connections (Iwasaki and Zheng, 2006). Based on the motor pattern measured using an electromyographic technique by Jayne and Lauder (Jayne and Lauder, 1995), these inhibitory connections in the reciprocal inhibition oscillator generate out-of-phase oscillations in the activities of the two neurons, which drive a pair of muscles

(i.e. anterior and posterior) alternately in sequence down to the tail on an ipsilateral side of the fish body. To ensure stable phase transition in the locomotor cycle to the contralateral side of the fish body, the afferent signals from different (at least two) channels of neurons innervating trunk SNs on the respective right and left sides of the fish body must appropriately be associated with each other in the central nervous system. Because of this characteristic feature of CPG-based control described above, we used unilateral ablation of sensory input from trunk SNs as experimental manipulation on the rationale that asymmetric disruption of sensory input may be particularly effective in demonstration of a sensory feedback component to central pattern generation for locomotion efficiency.

MATERIALS AND METHODS

Animals

Ninety-six juvenile *S. lalandi* were obtained from the Bream Bay Aquaculture Park, National Institute of Water and Atmospheric Research (NIWA), New Zealand. Fish were held in 3000 l tanks at the Leigh Marine Laboratory, and were fed three times a week on chopped fish, such as pilchard. The holding tanks were continuously aerated and flushed with high-quality filtered seawater. All the experiments were conducted under the approval of the University of Auckland Animal Ethics Committee (AEC application number R817).

Anatomical analysis of distribution of muscle fibres

Fish used for the measurements described in this section were starved for a period of 2 days and then euthanized with an overdose of MS-222 (100 mg ethyl 4-aminobenzoate per 1 l seawater). Five adult fish were selected in order to scale the mass of different muscle fibres. After the wetted mass of the fish was measured, each of the five specimens was submerged in 40°C water for 20 min so that the skin could easily be removed from the muscle. The mass of glycolytic (white) and oxidative (red and pink) muscle fibres were dissected separately from the fish body, and was immediately measured using an analytical balance. The mass of the remaining components, including bones, guts and skin, was also measured. The density of the dissected muscle groups containing oxidative (red + pink) and glycolytic (white) muscle was measured using the method of volumetric displacement. Nine adult fish were frozen for analysis of the distribution of the muscle fibres of different type. Each of the frozen specimens was first cut immediately behind the pectoral fin base, on average $30.4 \pm 1.8\%$ fork length (FL; mean \pm s.d.) from the snout, and then at standardized increments of 10% FL from 35 to 85% FL. Each transverse section was pictured using a digital camera (EX-F1, Casio, Tokyo, Japan), after which the areas of red, pink and white muscle were analysed with ImageJ (v1.43r, National Institutes of Health, MD, USA) and expressed as a percentage of the total muscle cross-sectional area.

Unilateral ablation of the lateral line

Mechanoreceptive patches of trunk SNs are aligned above the trunk lateral-line canal on the skin (Fig. 1). The SNs were ablated by a probe cooled by liquid nitrogen (Montgomery et al., 2003). This treatment was undertaken under anaesthetic induced with MS-222 (50 mg ethyl 4-aminobenzoate per 1 l seawater). A sham-treatment for lateral-line disruption was also made to evaluate the effects of anaesthetic, handling and associated treatments on swimming performance. The sham-treatment was performed in the same manner, but on an area of the body away from the SNs. The number of fish that received unilateral treatment on the left or right side of the body was the same within each group. Body morphometrics relevant to swimming performance, such as body length, depth and

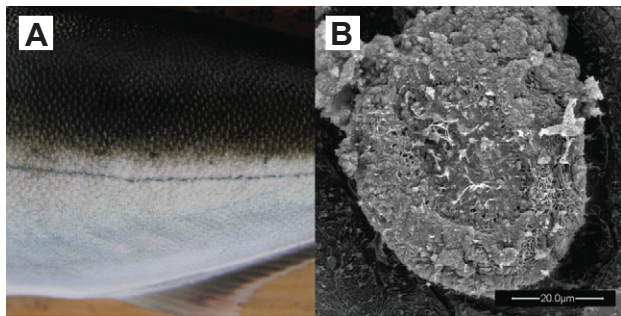


Fig. 1. The lateral line system of the yellowtail kingfish, *Seriola lalandi*. (A) Mechanoreceptive patches for superficial neuromasts are clearly visible as dark pigmented dots. The lateral-line canal including pores is visible as a dark line running horizontally across the body of the fish, in the middle of the picture. (B) Scanning electron micrograph of a superficial neuromast from a mature fish (fork length=0.362 m), showing the exposed cilia of the hair cells. The cupula is removed in the preparation process for electron microscopy.

width, were also recorded before fish were transferred to a recovery tank. The fish were allowed an additional 3–5 days before experimentation and the procedure was deemed successful if fish resumed feeding after a couple of hours. To minimise handling stress, ImageJ was used to estimate the fork length (FL) of control fish according to background grids placed in the working section of the flow chamber before the experimental trial. The body depth and width of the control fish was estimated using linear regressions obtained during preliminary measurements ($N=60$). If the true FL, depth and width measured at the end of the experiment differed from the estimated values, the flow velocity for the calculation of the critical swimming speed was corrected in the post-experimental analysis.

Critical swimming speed test protocol

The critical swimming speed (U_{crit}) test (Brett, 1964) has long been used to assess the prolonged swimming capacity of various species. U_{crit} is obtained from fishes subjected to incremental changes in speed over time in an experimental flow chamber. It is generally assumed that maximum oxygen uptake occurs at U_{crit} (Farrell and Steffensen, 1987; Farrell, 2007) and is thus a convenient way to measure both swimming performance and the maximum aerobic capacity of fish. Several investigators have found that U_{crit} overestimates sustained speed because recruitment of the fast-twitch, glycolytic muscle fibres at higher speeds is evident in a change in gait from a continuous tail beat to intermittent bursts of high-frequency tail beats followed by gliding (i.e. burst-and-glide) in the final stages of the U_{crit} test (Kolok, 1991; Webb, 1998). To avoid this discrepancy, Drucker (Drucker, 1996) proposed the gait transition speed (e.g. the speed at which pectoral fin locomotion is supplemented by body caudal fin locomotion) as an alternative cut-off swimming speed. Dickson et al. (Dickson et al., 2002) also defined the upper limit of scope for activity as swimming speed at which a continuous tail beat was shifted to a 'burst-and-glide' gait three times within 30 s. However, it is practically difficult to demonstrate the upper limit of scope for activity by counting how many times such gait shifts are conducted by the fish swimming in the swim tunnel within a certain period of time. Therefore, U_{crit} is considered to be a relatively robust and reliable metric for comparing the relative aerobic swimming capabilities of a body-caudal-fin swimmer such as *S. lalandi* (Williams and Brett, 1987; Hartwell and Otto, 1991; Peake and McKinley, 1998; Hogan et al., 2007).

The experiment commenced in late October 2010. At that time, the water temperature in the holding tanks was 18°C. Thirty-six fish were used for the U_{crit} test, divided into three groups: the control group (0.275 ± 0.043 m FL, $N=12$); a group that received sham treatment for SN disruption (sham SN-ablated fish: 0.277 ± 0.034 m FL, $N=12$); and an experimental group that received the treatment for SN disruption (SN-disrupted fish: 0.280 ± 0.027 m FL, $N=12$). Six individuals in each group were used for the respirometric measurement, and the other six individuals were used for kinematical measurements (reported separately). The U_{crit} test was carried out in a Brett-type swim tunnel (38.41) with a $0.16\times 0.16\times 0.55$ m (width \times height \times length) working section, where the flow was rectified by passing the water through a square mesh filter placed upstream in order to ensure a high degree of homogeneous and unidirectional flow. The downstream end of the working section was closed by a metal grid. During the test, fish swimming behaviour was recorded by two video cameras (EX-F1, Casio, Tokyo, Japan) that were set directly and obliquely above the working section of the respirometry flow chamber. The respirometry flow chamber was submerged in a water bath. The water was pumped from an experimental sump up to the water bath via an in-line water chiller (HC-1000A, Hailea, Guandong, China). A flushing pump was able to swap the water inside the respirometry flow chamber with water from the temperature controlled water bath. The water flow was generated by a frequency-modulated induction motor that was controlled with a frequency inverter (CFW-10, WEG, Scoresby, VIC, Australia). The flow velocity was controlled using customized software that altered the frequency of the power supply to the motor. The experimental flow system was surrounded by a plastic black-out sheet to prevent the fish from being disturbed. Supplementary fluorescent light was provided in the U_{crit} tests.

The experimental water temperature was maintained at 18–19°C during the experiment, although water temperature in the holding tanks did increase up to 21°C until the experiment finished in early March 2011. The slight discrepancy in the holding and experimental temperatures over the short period is not likely to have influenced our findings. At the start of the experiment, an individual fish was introduced to the swimming section of the swim flume and left to swim overnight (14–16 h) while taking respirometric measurements in a flow set to 0.7 forklengths (FL) s^{-1} . Fish were only used once in the experiments to preclude any effect of prior experience (Liao, 2006). Once fish were acclimated to the swim flume, the flow velocity was elevated to 1.0 FL s^{-1} . The flow speed, and thus the swimming speed, was increased by 0.3 FL s^{-1} every 30 min until the fish failed to swim by fatigue, and U_{crit} was interpolated from this final level of swimming performance [i.e. incremental velocity test (Brett, 1964; Jones, 1982; Farrell, 2007)]. In the present study, we assumed that fatigue was reached when the accumulated time that the body or fin of fish touched the downstream grid reached 1 min.

The absolute value of U_{crit} in ms^{-1} is dependent upon the length of fish. Therefore, U_{crit} was normalized by FL of the fish (Beamish, 1978) and was calculated as follows:

$$U_{crit} = U_{max} + (t_f/t_i)U_i, \quad (1)$$

where U_i is the velocity increment (0.3 FL s^{-1}), U_{max} is the maximum speed at which the fish was able to complete a 30-min period of swimming, t_f is the elapsed time from the velocity increase to fatigue and t_i is the time between the velocity increments (Brett, 1964). The presence of the fish in the enclosed chamber results in an increase in water velocity around the fish. Due to this phenomenon, the so-

called solid blocking effect, the flow velocity that the fish was exposed to was corrected in accordance with the equation described by Bell and Terhune (Bell and Terhune, 1970):

$$U = U_w(1 + A_f/A_c), \quad (2)$$

where U is corrected velocity, U_w is the flow velocity without fish, A_c is the cross-sectional area of the flow chamber and A_f is the cross-sectional area of the fish. A_f was approximated by an ellipse with the maximum depth of the body for the major axis (d) and the maximum width of the body for the minor axis (w), and was described as:

$$A_f = \delta dw/4. \quad (3)$$

Respirometric measurements and analysis

The mass-specific rate of oxygen consumption (\dot{M}_{O_2}) of 18 fish was resolved during U_{crit} swimming tests (see above for details on acclimation and flow velocity increments, etc.) to assess the swimming energetics of fish with intact and non-intact lateral lines: control group (0.304 ± 0.022 m FL, $N=6$); sham SN-disrupted fish (0.308 ± 0.011 m FL, $N=6$) and SN-disrupted fish (0.301 ± 0.008 m FL, $N=6$). The respirometer ran with a single measurement cycle consisting of three periods (i.e. flushing, waiting and measuring) according to the protocol of Steinhausen et al. (Steinhausen et al., 2005) and Brown et al. (Brown et al., 2011). During the flushing period, the flushing pump was active to mix the water inside the respirometry flow chamber and to ensure proper flow past the oxygen sensor. The flushing period (2–7 min) was changed depending on the fish and swimming speed so that the air saturation level of water would be $\sim 100\%$ at the end of the flushing period. During waiting and measuring periods, the flushing pump was turned off and the respirometry flow chamber was closed by a solenoid valve to prevent water from entering from an ambient tank. Before starting a new measuring period, a waiting period is necessary to account for a lag in the system response, resulting in a non-linear declination change in oxygen saturation of the water inside the respirometry flow chamber over the elapsed time. To avoid any risk of hypoxia developing, the length of the waiting and measuring periods were also modified to ensure air saturation never dipped below 80% saturation by the end of the measuring period. In general, however, measurement cycles were either 10 or 15 min, allowing two to three \dot{M}_{O_2} measurements for an individual fish swimming at each flow velocity.

The change in oxygen saturation over time, and hence \dot{M}_{O_2} , was measured at 1 Hz with a needle-type oxygen sensor (NTH-PS1-L5-TS-NS40/1.2-YOP, PreSens Precision, Regensburg, Germany) connected to a Microx-TX3 oxygen meter (PreSens Precision). The entire respirometer was under the control of customized software that not only managed water flow velocity but also initiated the flush, wait and measure cycle and recorded water O_2 saturation. The software then calculated the rate of change in water saturation per second (slope of the linear regression of oxygen saturation over the elapsed time), and this value was converted to \dot{M}_{O_2} ($\text{mg } O_2 \text{ kg}^{-1} \text{ min}^{-1}$) (*sensu* Steffensen, 1989) using the equation:

$$\dot{M}_{O_2} = \frac{(\Delta \text{sat} / 100) \times P_{O_2} \times \beta_{wO_2} \times v_w \times 60}{M}, \quad (4)$$

where Δsat is the recorded change in the percent of air saturation per second, P_{O_2} is the measured partial pressure of oxygen at 100% air saturation, β_{wO_2} is the capacitance coefficient of oxygen in water at a certain salinity ($0.369 \text{ mg } O_2 \text{ l}^{-1} \text{ kPa}$ at 36 p.p.t. for this experiment), V_w is the volume of the respirometer, 60 is the number of seconds in a minute and M is the mass of the fish.

\dot{M}_{O_2} was described as a power function of swimming speed (Steinhausen et al., 2005), U (FL s^{-1}) and M (kg) by:

$$\dot{M}_{O_2} = aM^{-0.2} + bM^{0.2}U^c. \quad (5)$$

Oxygen consumption data were fitted to the curve (Eqn 5) by the least-square method (generalized reduced gradient nonlinear algorithm, Microsoft Excel Solver, Microsoft, Redmond, WA, USA) in order to estimate the model parameters a , b and c . To account for variations in \dot{M}_{O_2} due to size differences amongst the fish, Clarke and Johnston (Clarke and Johnston, 1999) used the mass-specific exponent of $M^{(0.8-1)}$, thus $M^{-0.2}$ describes the allometric relationship between the standard metabolic rate (SMR) and mass of 69 species of teleost fish. SMR represents the energy required to maintain basic biological functions independent of activity, digestion or the costs of physiological stressors. The SMR was extrapolated as the oxygen consumption at zero swimming speed ($U=0$) using Eqn 5. To compare the cost of swimming as work per metre (WPM; J m^{-1}), \dot{M}_{O_2} was recalculated with the units $\text{mg } O_2 \text{ s}^{-1}$ and multiplied by a general oxycaloric value of $14.1 \text{ J mg}^{-1} O_2$ (Videler, 1993). The gross cost of transport (GCOT) is the value of WPM that is corrected for size effects by dividing by body weight (N) (Videler, 1993). GCOT ($\text{J N}^{-1} \text{ m}^{-1}$) at U_{opt} is therefore given by:

$$\text{GCOT} = \text{AMR}_{opt} (MgU_{opt})^{-1}, \quad (6)$$

where AMR_{opt} (J s^{-1}) is the active metabolic rate at the optimum swimming speed, U_{opt} , and g is the acceleration due to gravity (m s^{-2}). After Steinhausen et al. (Steinhausen et al., 2005), using the relationship between U and GCOT with Eqn 5 and 6, the optimum swimming speed, U_{opt} , where WPM is at its minimum, was obtained as:

$$U_{opt} = [a/b(c-1)]^{1/c}. \quad (7)$$

The level of metabolism available for locomotion (aerobic metabolic scope for activity) is usually calculated as the difference between SMR and AMR_{max} . AMR_{max} generally occurs at U_{crit} , and the fractional difference of AMR_{max} to SMR rate from this point onwards is referred to as factorial metabolic scope (FMS) (Fry, 1957):

$$\text{FMS} = \text{AMR}_{max} / \text{SMR}. \quad (8)$$

Composition of unsteady swimming

The acceleration and deceleration of fish swimming within the test section of the swim flume is a good indicator of steady (aerobic) *versus* unsteady (anaerobic) activity, the latter being more energetically expensive to maintain (Boisclair and Tang, 1993). The oxygen consumption of unsteady swimming was therefore analysed to address how swimming style might influence the respirometric measures of SN- and non-SN-disrupted fish.

The geometric centre of the fish swimming at all water velocities was tracked for 30 min at 30 Hz using open source video-tracking software SwisTrack ver. 4.1 (Correll et al., 2006), and the change in the rate of longitudinal displacement velocity was calculated, with final transformation to an acceleration unit with respect to fish length (FL s^{-2}). We categorized unsteady swimming activity into three levels: (1) one or more fork lengths acceleration ($\geq 1 \text{ FL s}^{-2}$), (2) less than one fork length acceleration ($< 1 \text{ FL s}^{-2}$) and (3) deceleration. However, even if the fish held the station of the body relative to the flow chamber, it is difficult to determine zero acceleration because the geometric centre was somewhat deflected (both longitudinally and laterally) due to body roll, changes in swimming depth and body tilt, etc. We therefore defined swimming as steady

if the rate of longitudinal displacement was within 10% FL (i.e. $\pm 0.1 \text{ FL s}^{-2}$).

Statistics

Basic statistics and pairwise tests were performed using the Analysis ToolPak of Microsoft Excel 2010. The statistical program R (ver. 2.12.2, R Development Core Team, Vienna, Austria) was used to run ANCOVA and multiple group comparisons with *post hoc* analysis. The effect of unilateral disruption on U_{crit} and respirometric performance was examined further if ANCOVA determined any significant difference in the following pairwise comparisons: (1) between control and SN-disrupted groups and (2) between sham SN-disrupted and SN-disrupted groups. Given statistical significance for the above pairwise comparisons, an insignificant result was desired for the comparison between control and sham SN-disrupted groups in order to support equivalence of the effect of unilateral disruption for control and sham SN-disrupted groups. In this scenario, the significance limit of an *F*-statistic was adjusted by Bonferroni correction in order to reduce the risk of Type I errors. If not stated otherwise, values are presented as means \pm s.d.

RESULTS

Distribution of muscle fibres

The mean mass of the whole lateral muscle was $0.4065 \pm 0.0941 \text{ kg}$ ($N=5$), and this corresponded to 52.3% of the body mass of the fish. The mean mass of oxidative (red + pink) and glycolytic (white) muscle was $0.0291 \pm 0.0060 \text{ kg}$ ($N=5$) and $0.3774 \pm 0.0886 \text{ kg}$ ($N=5$), which corresponded to 7.2 and 92.8% of whole muscle mass, respectively (Table 1). Red muscle was concentrated along the lateral line but penetrated the white muscle, and even reached the vertebral column along the horizontal septum (Fig. 2A). The change of muscle distribution along the body axis and the proportions of the red and pink muscle to the whole lateral muscle are shown in Fig. 2B. The areas of red and white muscle both reached a maximum at 35.0% FL from the snout (red: 80 mm^2 and white: 2282 mm^2). The area of the pink muscle reached a maximum at 45.0% FL from the snout (48 mm^2). The proportion of the oxidative red and pink muscle increased posteriorly, but the pink muscle was indistinguishable in most of the cross-sections from 75 to 85% FL from the snout. Oxidative muscle for the 75 and 85% FL sections could possibly contain pink muscle, but the ratio is so small it was deemed insignificant. A sharp increase in the proportion of the area of red muscle in the area of the whole muscle was found in the cross-sections posterior to 65% FL from the snout. The percentage of oxidative red muscle posterior to 65% FL was significantly greater than that in the anterior part (i.e. 30.4–45.0% FL from the snout) (Kruskal–Wallis test, $H=48.80$, d.f.=6, $P<0.01$,

followed by a *post hoc* Steel–Dwass test, $P<0.05$). In contrast, the proportion of the white muscle in the area of the whole muscle decreased posteriorly.

Critical swimming speed

The mean critical swimming speed (\bar{U}_{crit}) of the unilaterally SN-disrupted fish group was $2.11 \pm 0.96 \text{ FL s}^{-1}$ ($N=12$), and was significantly slower than the $3.66 \pm 0.19 \text{ FL s}^{-1}$ \bar{U}_{crit} ($N=12$) of sham SN-disrupted fish group (ANCOVA, $F_{1,21}=31.87$, $P<0.01$; Fig. 3). The \bar{U}_{crit} of control fish group was $3.89 \pm 0.45 \text{ FL s}^{-1}$ ($N=12$; Fig. 3), which was the fastest \bar{U}_{crit} of the three. No significant difference in FL was detected between the three groups (ANOVA, $F_{2,33}=0.07$, $P>0.05$). The U_{crit} in the control group was negatively correlated with the FL (two-tailed Spearman's rank correlation, $t=3.48$, d.f.=10, $P<0.01$). It might be expected that ability of the smaller fish to execute burst-and-coast gait swimming would be less restricted by the size of the flow chamber, resulting in a faster U_{crit} (Castro-Santos, 2004; Castro-Santos, 2005; Peake and Farrell, 2006; Tudorache et al., 2007). However, the \bar{U}_{crit} , from which this extraneous influence depending on the fish length was removed, was not significantly different between control and sham SN-disrupted fish groups (ANCOVA, $F_{1,21}=3.79$, $P>0.05$).

The mean maximum swimming speed (\bar{U}_{max}) was $3.79 \pm 0.42 \text{ FL s}^{-1}$ ($N=12$) for control fish and $3.60 \pm 0.21 \text{ FL s}^{-1}$ ($N=12$) for sham SN-disrupted fish. There was no significant difference between these two \bar{U}_{max} values (ANCOVA, $F_{1,21}=2.99$, $P>0.05$). However, the \bar{U}_{max} for SN-disrupted fish was lower, at $1.99 \pm 0.97 \text{ FL s}^{-1}$ ($N=12$), significantly slower than that for control (ANCOVA, $F_{1,21}=33.25$, $P<0.01$) and sham SN-disrupted fish (ANCOVA, $F_{1,21}=32.20$, $P<0.01$).

Respirometric measurement

Basic statistics describing the respirometric measures are given in Table 2. There was no significant difference in the FL and body mass between control, sham SN-disrupted and SN-disrupted fish groups (ANOVA, FL: $F_{2,15}=0.19$, mass: $F_{2,15}=0.41$, $P>0.05$), and so any difference reported herein is not due to body size effects. As shown in Fig. 4A, \dot{M}_{O_2} for sham SN-disrupted fish group was almost identical to the control group \dot{M}_{O_2} at all swimming speeds. A significant linear correlation between the logarithm of the \dot{M}_{O_2} and the swimming speed was found, but there was no significant difference in $\log \dot{M}_{\text{O}_2}$ between control and sham SN-disrupted fish groups (ANCOVA, $F_{1,138}=0.27$, $P>0.05$). The relationship between \dot{M}_{O_2} and swimming speed (U) was expressed by $\dot{M}_{\text{O}_2}=1.75M^{-0.2}+0.27M^{-0.2}U^{2.3}$ ($R^2=0.77$, $F_{1,143}=493.00$, $P<0.01$) for the control group and $\dot{M}_{\text{O}_2}=1.91M^{-0.2}+0.16M^{-0.2}U^{2.7}$ ($R^2=0.77$, $F_{1,148}=500.81$, $P<0.01$) for the sham SN-disrupted fish. The

Table 1. Mass of glycolytic white and oxydative (red + pink) muscle and relative percentage of the mass of the yellowtail kingfish

Individual	FL	Wet mass (kg)	White muscle mass (kg) [% relative to whole muscle mass]	Oxidative (red + pink) muscle mass (kg) [% relative to whole muscle mass]	Whole muscle mass (white + red + pink) [% relative to wet mass]	Remaining mass (kg) [% relative to wet mass]	Lost mass (kg) after measurement [% relative to wet mass]
1	0.357	0.601	0.247 [92.8]	0.019 [7.2]	0.266 [44.3]	0.325 [54.1]	0.010 [1.6]
2	0.393	0.871	0.422 [93.5]	0.029 [6.5]	0.452 [51.8]	0.403 [46.2]	0.017 [2.0]
3	0.404	0.915	0.481 [93.3]	0.035 [6.7]	0.516 [56.4]	0.378 [41.3]	0.021 [2.3]
4	0.365	0.684	0.341 [92.0]	0.030 [8.0]	0.370 [54.1]	0.296 [43.3]	0.018 [2.6]
5	0.386	0.813	0.395 [92.3]	0.033 [7.7]	0.428 [52.6]	0.379 [46.6]	0.007 [0.8]
Mean	0.381	0.777	0.377 [92.8]	0.029 [7.2]	0.407 [52.3]	0.356 [45.9]	0.014 [1.8]
s.d.	0.020	0.131	0.089 [0.6]	0.006 [0.6]	0.094 [4.6]	0.044 [4.9%]	0.006 [0.7]

FL, fork length.

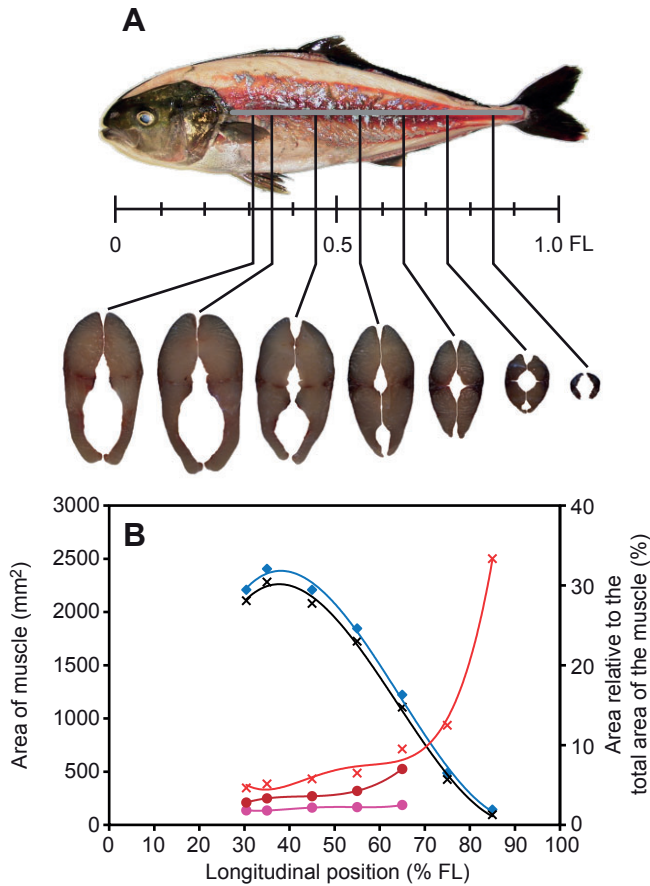


Fig. 2. Distribution of the mean area of red, pink and white muscle and the percent of the area relative to the whole muscle area. (A) Lateral view of the distribution of the red muscle and transverse sections. (B) The absolute area of the white (black crosses) and whole muscle (blue diamonds), and percent of areas of different fibre type relative to the whole muscle area for the oxydative red + pink (red crosses), red (red circles) and pink (pink circles) muscle at different longitudinal positions. The mean area of each muscle type was adjusted by the area *versus* FL² relationship (ANCOVA) to account for allometry effects. The curves (fourth-order polynomials) are indicated for illustration purposes only. FL, fork length.

intercept of the model curve with the vertical axis (Fig. 4A) was determined as the SMR. The estimated SMR values for control and sham SN-disrupted fish groups were 2.16 and 2.32 mg O₂ kg⁻¹ min⁻¹, respectively. Because the SN-disrupted fish exhibit a high rise in \dot{M}_{O_2} between 0.7 and 1.3 FL s⁻¹ (Fig. 4B), their extrapolated SMR was unreasonably underestimated. Because SN ablation should not affect SMR, it was assumed that the SMR of the SN-disrupted fish was the same as that of the sham SN-disrupted fish group for the model fitting process (Fig. 4B). This assumption allowed the \dot{M}_{O_2} of SN-disrupted fish group to be reasonably described by $\dot{M}_{O_2} = 1.88M^{0.2} + 0.97M^{0.2}U^{1.4}$ ($R^2 = 0.53$, $F_{1,91} = 103.33$, $P < 0.01$). This correction revealed a significant difference in \dot{M}_{O_2} between sham SN-disrupted and SN-disrupted fish groups in the swimming speed range of 1.0–2.2 FL s⁻¹ (ANCOVA, $F_{1,65} = 10.71$, $P < 0.01$), where 2.2 FL s⁻¹ was the closest swimming speed to the mean U_{crit} of SN-disrupted fish group. It is important to note that only one SN-disrupted fish could complete two cycles of the \dot{M}_{O_2} measurement during the 3.4 FL s⁻¹ velocity swimming, and recorded \dot{M}_{O_2} values statistically similar to those for the other two groups (ANOVA, $F_{2,20} = 0.95$, $P > 0.05$; Fig. 4B):

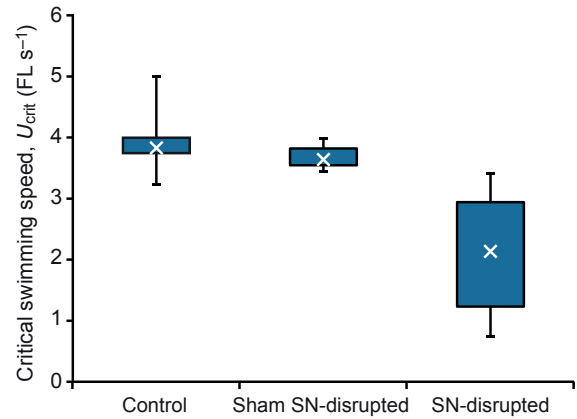


Fig. 3. Box-plot of critical swimming speed. Boxes are defined by the first and third quartile values, and the total ranges of values ($N = 12$) are shown as vertical bars. The white crosses represent median U_{crit} values. SN, superficial neuromast.

8.6 ± 1.3 mg O₂ kg⁻¹ min⁻¹ (10 measurements) for control fish, 8.3 ± 1.1 mg O₂ kg⁻¹ min⁻¹ (11 measurements) for sham SN-disrupted fish and 9.5 ± 0.2 mg O₂ kg⁻¹ min⁻¹ (two measurements) for SN-disrupted fish.

The mean AMR at U_{max} (\overline{AMR}_{max}) was 8.76 ± 1.60 mg O₂ kg⁻¹ min⁻¹ for control fish ($N = 6$) and 9.23 ± 1.19 mg O₂ kg⁻¹ min⁻¹ for sham SN-disrupted fish ($N = 6$). The \overline{AMR}_{max} for SN-disrupted fish was 7.47 ± 3.29 mg O₂ kg⁻¹ min⁻¹ ($N = 6$). This was the lowest \overline{AMR}_{max} of the three groups, but there was no significant difference between the three \overline{AMR}_{max} values (one-way ANOVA, $F_{2,15} = 1.01$, $P > 0.05$). The mean FMS (FMS) for the SN-disrupted fish (2.87 ± 0.78, $N = 6$) was significantly less than that of control fish (4.04 ± 0.75, $N = 6$) and sham SN-disrupted fish (4.14 ± 0.37, $N = 6$; one-way ANOVA, $F_{2,15} = 6.80$, $P < 0.05$, followed by a Tukey's *post hoc* HSD multiple comparison test, $P < 0.05$). There was no significant difference in FMS between control and sham SN-disrupted fish (one-way ANOVA, $F_{2,15} = 6.80$, $P < 0.01$, followed by a Tukey's *post hoc* HSD multiple comparison test, $P > 0.05$).

The mean GCOT of fish in the control and sham SN-disrupted groups was also almost identical at each swimming speed (Fig. 5A) and reflects similarity in the \dot{M}_{O_2} –swim-speed relationship (above). The mean GCOT of SN-disrupted fish, however, was significantly greater than that of sham SN-disrupted fish at swimming speeds from 1.0 to 2.2 FL s⁻¹ (ANCOVA, $F_{1,65} = 14.43$, $P < 0.01$; Fig. 5B). The U_{opt} that was extrapolated using the power model (i.e. Eqns 5, 7) was 2.0 FL s⁻¹ for both control and sham SN-disrupted fish. Using the same approach, a U_{opt} value of 2.7 FL s⁻¹ was obtained for SN-disrupted fish. The corresponding value of GCOT_{min} at U_{opt} (calculated from Eqn 6 using the mean mass of each group) was similar between control fish (0.15 JN⁻¹ m⁻¹) and sham-disrupted fish (0.14 JN⁻¹ m⁻¹), but was approximately 1.5 times greater for SN-disrupted fish (0.22 JN⁻¹ m⁻¹).

In addition to the overall power model estimations (above), the mean optimal swimming speed (\overline{U}_{opt}) obtained from individual fish was estimated to be 2.25 ± 0.50 FL s⁻¹ ($N = 6$) for control fish, 2.00 ± 0.70 FL s⁻¹ ($N = 6$) for sham SN-disrupted fish and 1.70 ± 0.81 FL s⁻¹ ($N = 6$) for SN-disrupted fish. Although the overall difference in \overline{U}_{opt} between the three groups was not significant (one-way ANOVA, $F_{2,15} = 0.96$, $P > 0.05$), the mean GCOT at U_{opt} (GCOT_{min}) of SN-disrupted fish (0.18 ± 0.06 JN⁻¹ m⁻¹, $N = 6$) was significantly greater than that of the other two groups (one-way

Table 2. Basic statistics from the respirometric measurement (mean \pm s.d., $N=6$) of the yellowtail kingfish

	Control fish	Sham SN-disrupted fish	SN-disrupted fish
Fork length, FL (m)	0.304 \pm 0.022	0.308 \pm 0.011	0.301 \pm 0.008
Mass, M (kg)	0.347 \pm 0.070	0.366 \pm 0.051	0.340 \pm 0.026
Standard metabolic rate, SMR (mg O ₂ kg ⁻¹ min ⁻¹)	2.16	2.32	2.32
Maximum metabolic rate, AMR _{max} (mg O ₂ kg ⁻¹ min ⁻¹)	8.76 \pm 1.60	9.23 \pm 1.19	7.47 \pm 3.29
Optimal swimming speed, U_{opt} (FL s ⁻¹)	2.25 \pm 0.50 (2.00)	2.00 \pm 0.70 (2.00)	1.70 \pm 0.81 (2.74)
Gross cost of transport, GCOT (J N ⁻¹ m ⁻¹)	0.10 \pm 0.03 (0.15)	0.11 \pm 0.03 (0.14)	0.18 \pm 0.06* (0.22)
Factorial metabolic scope, FMS	4.04 \pm 0.75	4.14 \pm 0.37	2.87 \pm 0.78**
Maximum swimming speed, U_{max} (FL s ⁻¹)	3.79 \pm 0.42	3.60 \pm 0.21	1.99 \pm 0.97**

The SMR of superficial neuromast (SN)-disrupted fish was assumed to be the same as that of sham SN-disrupted fish group.

*Significant at $P<0.05$; **significant at $P<0.01$.

The values in parentheses represent the estimates based on a power model of mass-specific oxygen consumption (\dot{M}_{O_2}), $\dot{M}_{O_2}=aM^{-0.2}+bM^{-0.2}U^c$, where parameters a , b and c are estimated from data, and M is the mean mass of the fish for each group.

ANOVA, $F_{2,15}=4.28$, $P<0.05$, followed by a Tukey's *post hoc* HSD multiple comparison test, $P<0.05$). The \overline{GCOT}_{min} was comparable between control (0.10 \pm 0.03 J N⁻¹ m⁻¹, $N=6$) and sham SN-disrupted fish (0.11 \pm 0.03 J N⁻¹ m⁻¹, $N=6$; one-way ANOVA, $F_{2,15}=4.28$, $P<0.05$, followed by a *post hoc* Tukey's HSD multiple comparison test, $P>0.05$). Contrary to the overall power model estimate of U_{opt}

(i.e. 2.7 FL s⁻¹), the \overline{U}_{opt} for SN-disrupted fish was significantly slower than the \overline{U}_{crit} of this group (Friedman test, $\chi^2=7.00$, d.f.=2, $P<0.05$, followed by a *post hoc* Scheffe's method for pairwise comparison, $P<0.05$), but it was not significantly different from the \overline{U}_{max} of this group (Friedman test, $\chi^2=7.00$, d.f.=2, $P<0.05$, followed by a *post hoc* Scheffe's method for pairwise comparison, $P>0.05$).

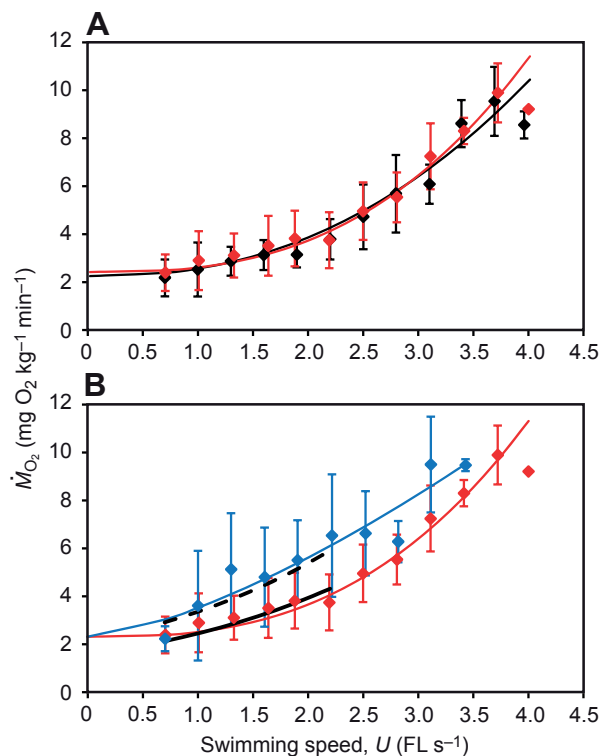


Fig. 4. Comparison of mass-specific oxygen consumption (\dot{M}_{O_2}) between fish groups with and without a unilateral ablation of trunk superficial neuromasts (SNs). The plots compare \dot{M}_{O_2} (mean \pm s.d., \dot{M}_{O_2}) (A) between control (black) and sham SN-disrupted (red) fish groups and (B) between sham SN-disrupted (red) and SN-disrupted (blue) fish groups. The curves represent the power model $\dot{M}_{O_2}=aM^{-0.2}+bM^{-0.2}U^c$ for (A) control (black) and sham SN-disrupted (red) fish, and (B) sham SN-disrupted (red) and SN-disrupted (in blue) fish. The model parameters a , b and c are approximated from empirical data obtained from fish with mean body mass of M . The ANCOVA regression models of $\log(\dot{M}_{O_2})$ on the swimming speed ($U=1.0$ – 2.2 FL s⁻¹) for sham SN-disrupted (solid black curve) and SN-disrupted (dashed black curve) fish groups are compared in B. The error bars represent s.d. from a mean of $N=6$. FL, fork length.

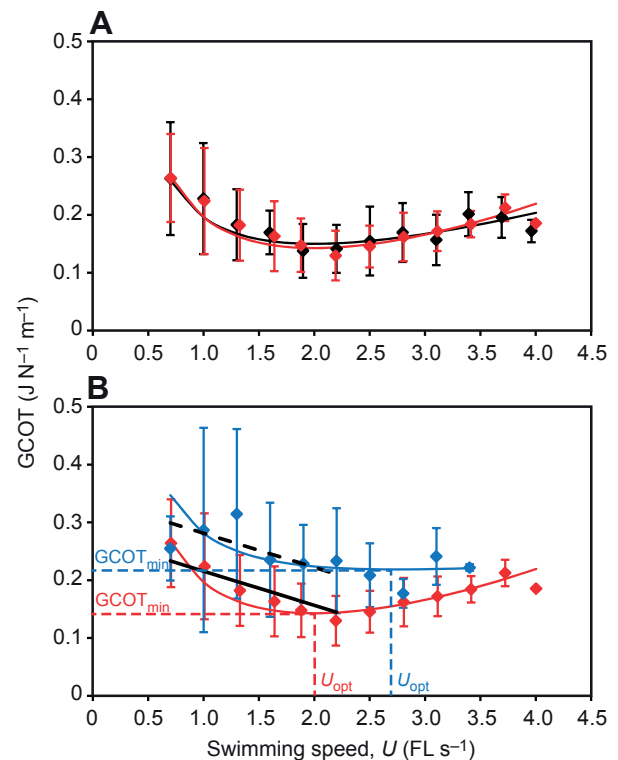


Fig. 5. Comparison of gross cost of transport (GCOT) between fish groups with and without a unilateral ablation of trunk superficial neuromasts (SNs). Plots compare GCOT (mean \pm s.d.) (A) between control (black) and sham SN-disrupted (red) fish groups and (B) between sham SN-disrupted (red) and SN-disrupted (blue) fish groups. The curves represent the model estimated from $\dot{M}_{O_2}=aM^{-0.2}+bM^{-0.2}U^c$ (A) for control (black) and sham SN-disrupted (red) and (B) for sham SN-disrupted (red) and SN-disrupted (blue) fish groups. The model parameters a , b and c are approximated from empirical data obtained from fish with mean body mass of M . The optimal swimming speed, U_{opt} , was determined based on the approximated GCOT curve where the cost of transport was minimal ($GCOT_{min}$). The ANCOVA regression models of GCOT on swimming speed ($U=1.0$ – 2.2 FL s⁻¹) for sham SN-disrupted (solid black curve) and SN-disrupted (dashed black curve) fish groups are compared in B. The error bars represent s.d. from a mean of $N=6$. FL, fork length.

Composition of unsteady swimming

For both control and sham SN-disrupted fish, the percent frequency of quasi-steady swimming (i.e. steady swimming or accelerations $<1.0 \text{ FL s}^{-2}$) was nearly twofold greater than the percent frequency of unsteady swimming (i.e. accelerations $\geq 1.0 \text{ FL s}^{-2}$) (two-way ANOVA, $F_{1,56}=48.07$, $P<0.01$ for control fish and $F_{1,48}=36.33$, $P<0.01$ for sham SN-disrupted fish; Fig. 6A,B). For SN-disrupted fish, however, quasi-steady and unsteady measures shared approximately equal frequencies (two-way ANOVA, $F_{1,34}=1.79$, $P>0.05$; Fig. 6C). The percentage frequency of all acceleration measures was generally independent of flow speed in all three groups (regression analysis for control fish: $F_{1,28}=0.81$, $P>0.05$; for sham SN-disrupted fish: $F_{1,27}=0.45$, $P>0.05$; for SN-disrupted fish: $F_{1,20}=0.34$, $P>0.05$). Most importantly, the average percentage frequency of unsteady activity ($\geq 1.0 \text{ FL s}^{-2}$) for the SN-disrupted fish was significantly greater than that for the control and sham SN-disrupted fish (two-way ANOVA, $F_{2,66}=4.88$, $P<0.05$; Fig. 7A). There were differences between the three groups in terms of quasi-steady swimming (two-way ANOVA, $F_{2,66}=3.86$, $P<0.05$; Fig. 7B); the percentage frequency of quasi-steady swimming by SN-disrupted fish was less than that of controls (*post hoc* Tukey's HSD multiple comparison test, $P<0.05$) but statistically similar to that of sham SN-disrupted fish (*post hoc* Tukey's HSD multiple comparison test, $P>0.05$). There was, however, no significant difference in the average percentage frequency of deceleration activity ($\leq -0.1 \text{ FL s}^{-2}$) between the three groups (two-way ANOVA, $F_{2,66}=1.37$, $P>0.05$; Fig. 7C).

DISCUSSION

Seriola lalandi muscle and its relationship with aerobic swimming performance

Myotomal muscle is the primary means of propulsion in fishes and, with slow oxidative (red) and fast glycolytic (white) muscle fibres being both anatomically and functionally separated, the proportional mix of muscle type is generally believed to reflect the swimming ecology of different species (Videler, 1993). Fishes power steady undulatory swimming with both red and pink muscle but recruit white glycolytic fibres when fast unsteady movements, such as sprint and burst swimming, are required (Rome et al., 1992; Coughlin and Rome, 1996; Ellerby and Altringham, 2001). Examining the relative proportion of the different muscle fibres thus provides a valuable insight into the routine swimming performance of different species. For instance, constant-swimming pelagic species generally have more slow muscle than benthic species (Videler, 1993; Ellerby and Altringham, 2001), and our analysis of muscle fibre allocations

certainly provides support for *S. lalandi* also being a fast-swimming cruiser. The percentage cross-sectional area of aerobic (red and pink) muscle in *S. lalandi* increased posteriorly, and the percentage for the posterior 65% of the body was significantly greater than the anterior 35%, suggesting that the red and pink muscle plays a very important role in carangiform swimming, where large lateral undulations are restricted to the posterior part of the body. It is probable that the pink muscle of *S. lalandi* is a fast-twitch muscle with contraction speeds lying somewhere between the performance of red and white fibres (Coughlin et al., 1996).

The total mass ratio of the oxidative red and pink muscle fibres was found to range from 6.5 to 8.0% in the whole muscle of *S. lalandi*, which, although less than common active pelagic species [e.g. sardine *Sardinopus melanostica*, 20.7% and chub mackerel *Scomber japonicus*, 12.0% (Obatake and Heya, 1985)], is considerably greater than that of common demersal species [e.g. yellow sea bream *Taivs tumifrons*, 2.2% and sillago *Sillago japonica*, 1.6% (Obatake and Heya, 1985)]. *Seriola lalandi* shows a red muscle mass ratio similar to that of the jack mackerel (*Trachurus japonica*), the latter having a red muscle fraction range of 7.7–8.6% (Obatake and Heya, 1985; Xu et al., 1993). The fact that both carangids have red muscle ratios in the vicinity of 6.5–8.6% suggests that this ratio is presumably sufficient to support rapid long-term schooling, a characteristic of both species. Examining the shift in muscle type along the length of carangiform and sub-carangiform modes of swimming lends further support to this argument. For example, in *S. lalandi*, the posterior bias for oxidative red and pink muscle fibres is clearly seen in Fig. 2A. The gadoid *Merlangius merlangus*, a sub-carangiform swimmer that has more body bending and does not solely create thrust from posterior sections, was found to have 2% red muscle at 35% of the body length and 14.3% at 79% of the body length (Greer-Walker and Pull, 1975). *Seriola lalandi* at similar positions in the present study (Fig. 2B) was found to have 5.1% oxidative fibres at 35% FL and 22.9% at 80% FL (if a linear correlation was assumed between the proportions at 75 and 85% FL). *Seriola lalandi* therefore shows features of a cruising specialist with a carangiform mode of swimming.

The use of fast carangid swimming by *S. lalandi* is also supported by our respirometry data. Active epipelagic species are generally seen to have high SMR to maintain swimming machinery supporting peak performance at high AMR_{max} (Benetti et al., 1995). Clark and Seymour (Clark and Seymour, 2006) measured the SMR of 2.1 kg *S. lalandi* at 20 and 25°C and derived values of 1.55 and 3.31 $\text{mg O}_2 \text{ kg}^{-1} \text{ min}^{-1}$, respectively. Their 1.55 $\text{mg O}_2 \text{ kg}^{-1} \text{ min}^{-1}$ SMR at 20°C corresponds to 2.22 $\text{mg O}_2 \text{ kg}^{-1} \text{ min}^{-1}$ for a 0.347 kg

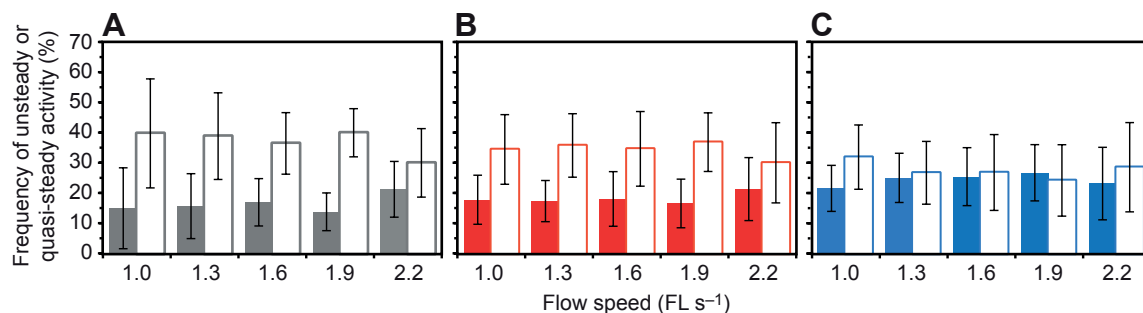


Fig. 6. Comparison of unsteady (solid bars) and quasi-steady (hollow bars) swimming activities within (A) control, (B) sham SN-disrupted and (C) SN-disrupted fish groups. The magnitude of acceleration was classified based on the rate of velocity increase per second: between -0.1 and 1.0 FL s^{-2} (quasi-steady), 1.0 FL s^{-2} or greater (unsteady) and less than -0.1 FL s^{-2} (decelerating). Percentage frequency equates to the number of acceleration events relative to the total number of movements made across the 30 min observation period. The error bars represent s.d. from a mean of $N=6$. FL, fork length.

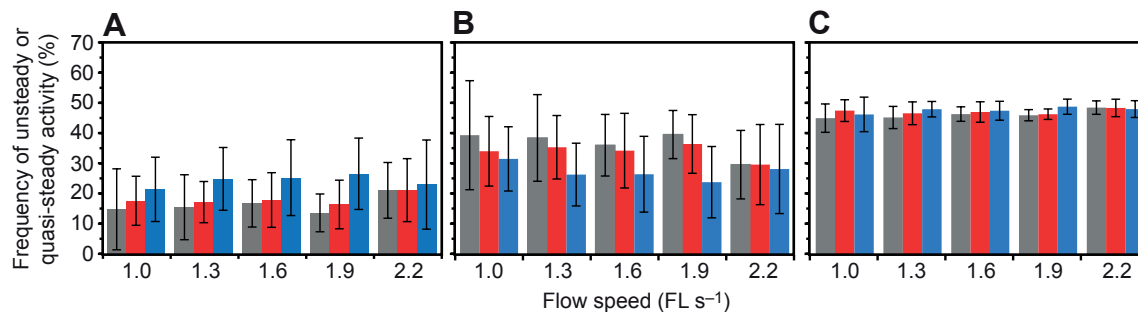


Fig. 7. Comparison of percentage frequency of (A) unsteady swimming activity, (B) quasi-steady swimming activity and (C) decelerating activity between control (grey bars), sham SN-disrupted (red bars) and SN-disrupted (blue bars) fish groups. The magnitude of acceleration was classified based on the rate of velocity increase per second: between -0.1 and 1.0 FL s^{-2} (quasi-steady), 1.0 FL s^{-2} or greater (unsteady) and less than -0.1 FL s^{-2} (decelerating). Percentage frequency equates to the number of acceleration events relative to the total number of movements made across the 30 min observation period. The error bars represent s.d. from a mean of $N=6$. FL, fork length.

fish if a mass-specific exponent of -0.2 is used (Clarke and Johnston, 1999). The $2.16 \text{ mg O}_2 \text{ kg}^{-1} \text{ min}^{-1}$ SMR of our 0.347 kg control fish at 18°C is therefore close to the measures of Clark and Seymour (Clark and Seymour, 2006). When looking at other pelagic carangids, the chub mackerel *Scomber japonicus* provides a good comparison of SMR because it is an epipelagic predator specialized for rapid and efficient swimming (Dickson et al., 2002). Dickson et al. (Dickson et al., 2002) reported an SMR of $2.11 \text{ mg O}_2 \text{ kg}^{-1} \text{ min}^{-1}$ for a 0.095 kg *S. japonicus* at 18°C . This measure of SMR is close to that of our control fish, but obviously applies to a smaller fish and is therefore less than that of our *S. lalandi* if a mass exponent of -0.2 is applied. The U_{opt} of control and sham treated fish within the current line of work was 2.0 FL s^{-1} at 18°C , which is directly comparable to 2.2 FL s^{-1} U_{opt} of *S. lalandi* at 22°C within the study of Brown et al. (Brown et al., 2011) using the same swim flume and similarly sized fish. However, other more sluggish species such as saithe and whiting are seen to have much lower U_{opt} values in the vicinity of 1.4 and 1.0 FL s^{-1} , respectively (Steinhausen et al., 2005). The specialized musculature and relatively high U_{opt} and SMR of *S. lalandi* therefore suggest that this species uses relatively faster swimming speed during routine moving and foraging, and it is within these more energy-demanding speeds that the lateral line is likely to play a more substantive role.

Effect of lateral-line disruption on aerobic metabolic capacity and mode of swimming

SN-disrupted fish had a lower swimming performance and swam less efficiently. Not only were they unable to attain high critical swimming speeds (Fig. 3), but across a comparable range of swimming up to the U_{crit} level of 2.11 FL s^{-1} , their rate of O_2 consumption per unit swimming speed was greater (Fig. 4B). Although \dot{M}_{O_2} was higher for SN-disrupted fish, the drop in U_{crit} swimming performance translated into a reduced aerobic scope, implying that fish were possibly forced to recruit anaerobic fibres earlier in the U_{crit} test. As illustrated in Fig. 5B, some SN-disrupted individuals would have had to swim beyond their U_{crit} limit to capitalize on the benefits of U_{opt} , their least costly swimming speed at 2.74 FL s^{-1} , which emphasizes the mismatch in swimming efficiency and performance in this group. Only one SN-disrupted fish could complete two cycles of the \dot{M}_{O_2} measurement at 3.4 FL s^{-1} , and showed \dot{M}_{O_2} measurements similar to those of the fish with intact lateral-line input (Fig. 4B). This may result from the stabilized swimming performance by multisensory substitution involving canal neuromasts, which have a higher threshold for hydrodynamic

stimuli (high-frequency flow). The estimated U_{opt} for control fish suggests that *S. lalandi* use swimming speeds as fast as 2 FL s^{-1} for routine swimming, such as during migration and foraging. These considerations taken together suggest that the upper limit of the swimming speed range where trunk SNs are responsible for motor control for swimming efficiency may fall between 2.0 and 3.4 FL s^{-1} . The fish with intact lateral lines were able to sustain swimming across an extended range of speeds and were able to capitalize on the benefit of the least costly swimming at U_{opt} . The results of the present study therefore suggest that the majority of SN-disrupted fish were subject to increased swimming costs and showed poor swimming efficiency and performance across a range of swimming speeds. In relation to the \dot{M}_{O_2} measures, no significant difference in GCOT was detected between fish with and without intact lateral lines when swimming at U_{opt} . This suggests that SN-disrupted fish are required to take the same period of time to reach the same distance if swimming at U_{opt} . This is the least costly swimming activity. However, SN-disrupted fish will subsequently consume 1.5 times greater aerobic energy compared with control and sham SN-disrupted fish. The higher GCOT at U_{opt} for SN-disrupted fish and shallower U-shaped relationship of GCOT with swimming speed (Fig. 5B) suggest that the cost of swimming for this group of fish was considerably high up to U_{crit} . That is because the difference between the GCOT at U_{opt} and U_{crit} was negligibly small despite the fact that the GCOT at swimming speeds around U_{crit} should arguably be high due to the exponentially increased hydrodynamic resistance that the fish had to overcome. It is essential that, like *S. lalandi*, fish species leading a pelagic life use the most cost-effective swimming speed (i.e. U_{opt}) for longer and more directional movement. Therefore, relatively inefficient swimming at U_{opt} must have substantial impact on their fitness components, such as survival, growth, reproduction and other relevant responses.

Behavioural aspects of swimming (i.e. steady versus unsteady manoeuvres of swimming; Figs 6, 7) analysed in the U_{crit} test obviously have important implications for the bioenergetics of swimming *S. lalandi*. It would appear that the greater GCOT of SN-disrupted fish was attributed to their frequent use of an unsteady swimming gait (i.e. $\geq 1.0 \text{ FL s}^{-2}$; Fig. 7A) and other spontaneous activities, such as turns, breaks and fin movements for stability control, that were observed in SN-disrupted fish during intermediate swimming between 1.0 and 1.9 FL s^{-1} . However, the percentage frequency of quasi-steady swimming (steady swimming or accelerations $< 1.0 \text{ FL s}^{-2}$) for SN-disrupted fish swimming at 2.2 FL s^{-1} was almost exactly the same as that for control and sham

SN-disrupted fish swimming at 2.2 FL s^{-1} . Nevertheless, the GCOT of SN-disrupted fish ($0.23 \text{ J N}^{-1} \text{ m}^{-1}$) swimming at 2.2 FL s^{-1} was significantly greater than that of control ($0.14 \text{ J N}^{-1} \text{ m}^{-1}$) and sham SN-disrupted fish ($0.13 \text{ J N}^{-1} \text{ m}^{-1}$) swimming at the same speed. We therefore believe that the relatively high level of inefficient/high-cost swimming seen in the SN-disrupted fish may have contributed to the elevated level of GCOT of this group.

Disrupting the lateral line of *S. lalandi* is seen to affect the mode of swimming in a way that increases the metabolic costs of travel. This potentially provides evidence for a role of flow-sensing feedback from trunk SNs on both sides of the fish body in swimming efficiency, but the mechanism by which this effect occurs is not yet resolved. One possibility is that SN-disrupted fish experienced an asymmetric disruption of sensory feedback from trunk SNs or asymmetric integration of mechanosensory input within the central nervous system that resulted in unsteady swimming and reduced swimming efficiency (Boisclair and Tang, 1993). We believe that this may have occurred and at least partially explains why U_{crit} swimming performance was reduced and O_2 consumption at standardized rates of swimming was higher in the SN-disrupted fish. The use of unsteady swimming undoubtedly produced a high-cost relationship between O_2 consumption and swimming speed in the SN-disrupted fish. Previous investigators have proposed a role for sensory feedback in promoting efficient kinematics (Lighthill, 1993) and boundary layer control (Anderson et al., 2001). However, more detailed studies of kinematics and boundary layer control after sensory manipulation are required to directly test these possibilities. Further work is also required to clarify whether there are other factors, such as changes in swimming behaviour, that contribute to the observed efficiency deficits created by SN ablation.

Previous studies have shown that CPGs are involved in generation of rhythmic neural output for diverse rhythmic activities in various animals, including swimming in fishes (Tytell and Cohen, 2008). It is also known that although CPGs produce a rhythmic motor pattern in the absence of any external cues (i.e. CPG-based control), deafferented animals were not able to sustain the rhythmic pattern of CPGs for long periods without sensory input, and that in a natural situation, a great number of afferent sensory inputs are involved in the sustained production of the rhythmic motor patterns (Belanger and Orchard, 1992; da Silva and Lange, 2011). Assuming that this is also the case in our *S. lalandi*, even if lateral-line input from trunk SNs was completely blocked by bilateral SN ablation, the alternative sensory feedback system could compensate for the perturbation that would otherwise be caused by the bilateral SN ablation, by performing a similar function. Therefore, we chose unilateral SN ablation as the experimental manipulation rather than bilateral ablation on the rationale that central pattern generation may be more sensitive to asymmetric disruption of sensory input. It is interesting to note that the observed change in metabolic and cost-of-transport measures is particularly evident at intermediate swimming speeds. One interpretation of these findings is that sensory feedback to modify CPGs for locomotion efficiency is more important over an intermediate swimming range. It is possible that the CPGs are tuned to operate efficiently at higher swimming speeds without sensory feedback from trunk SNs, and that it is at intermediate swimming speeds that active sensory feedback will be more evident.

LIST OF SYMBOLS AND ABBREVIATIONS

a, b, c	parameters in a power function of swimming speed and body mass for oxygen consumption
A_c	cross-sectional area of the flow chamber
A_f	cross-sectional area of the fish

AMR	active metabolic rate
AMR_{max}	maximum active metabolic rate
$\overline{\text{AMR}}_{\text{max}}$	mean maximum active metabolic rate
AMR_{opt}	active metabolic rate at optimal swimming speed
CPG	central pattern generator
d	maximum depth of the fish body
FL	fork length of the fish
FMS	fractional metabolic scop
$\overline{\text{FMS}}$	mean FMS
GCOT	gross cost of transport
GCOT_{min}	minimum GCOT based on a power model of \dot{M}_{O_2}
$\overline{\text{GCOT}}_{\text{min}}$	mean minimum GCOT
g	gravitational acceleration
M	mass of the fish
\dot{M}_{O_2}	mass-specific oxygen consumption rate
P_{O_2}	partial pressure of oxygen at 100% air saturation
SMR	standard metabolic rate
SN	superficial neuromasts
t_f	elapsed time from the velocity increase to fatigue of the fish in the U_{crit} test
t_i	time between the velocity increments in the critical swimming speed test
U	flow velocity or swimming speed when the fish held its station relative to the flume
U_{crit}	critical swimming speed
$\overline{U}_{\text{crit}}$	mean critical swimming speed
U_i	velocity increment in the U_{crit} test
U_{max}	maximum swimming speed at which the fish was able to complete 30-min period of swimming in the U_{crit} test
$\overline{U}_{\text{max}}$	mean maximum swimming speed
U_{opt}	optimal swimming speed based on a power model of \dot{M}_{O_2}
$\overline{U}_{\text{opt}}$	mean optimal swimming speed
U_w	flow velocity without fish
V_w	volume of the respirometer
WPM	cost of swimming as work per metre
β_{wO_2}	capacitance coefficient of oxygen in water at a certain salinity
Δsat	change in % of air saturation per second

FUNDING

This study was financially supported by the New Zealand Foundation of Research Science and Technology (FRST) under the Fellowship Program jointly administrated by the Japan Society for Promotion of Science (JSPS).

REFERENCES

- Anderson, E. J., McGillis, W. R. and Grosenbaugh, M. A. (2001). The boundary layer of swimming fish. *J. Exp. Biol.* **204**, 81-102.
- Beamish, F. W. H. (1978). Swimming capacity. In *Fish Physiology*, Vol. 7 (ed. W. S. Hoar and D. J. Randall), pp. 101-187. New York: Academic Press.
- Belanger, J. H. and Orchard, I. (1992). The locust ovipositor opener muscle: proctolinergic central and peripheral neuromodulation in a centrally driven motor system. *J. Exp. Biol.* **174**, 343-362.
- Bell, W. H. and Terhune, L. D. B. (1970). Water tunnel design for fisheries research. *J. Fish. Res. Board Can. Tech. Rep.* **195**, 1-69.
- Benetti, D. D., Brill, R. W. and Kraul, S. A., Jr (1995). The standard metabolic rate of dolphin fish. *J. Fish Biol.* **46**, 987-996.
- Boisclair, D. and Tang, M. (1993). Empirical analysis of the influence of swimming pattern on the net energetic cost of swimming in fishes. *J. Fish Biol.* **42**, 169-183.
- Brett, J. R. (1964). The respiratory metabolism and swimming performance of young sockeye salmon. *J. Fish. Res. Board Can.* **21**, 1183-1226.
- Brown, E. J., Bruce, M., Pether, S. and Herbert, N. A. (2011). Do swimming fish always grow fast? Investigating the magnitude and physiological basis of exercise-induced growth in juvenile New Zealand yellowtail kingfish, *Seriola lalandi*. *Fish Physiol. Biochem.* **37**, 327-336.
- Brown, T. G. (1911). The intrinsic factors in the act of progression in the mammal. *Proc. R. Soc. Lond. B* **84**, 308-319.
- Castro-Santos, T. (2004). Quantifying the combined effects of attempt rate and swimming performance on passage through velocity barriers. *Can. J. Fish. Aquat. Sci.* **61**, 1602-1615.
- Castro-Santos, T. (2005). Optimal swim speeds for traversing velocity barriers: an analysis of volitional high-speed swimming behavior of migratory fishes. *J. Exp. Biol.* **208**, 421-432.
- Clark, T. D. and Seymour, R. S. (2006). Cardiorespiratory physiology and swimming energetics of a high-energy-demand teleost, the yellowtail kingfish (*Seriola lalandi*). *J. Exp. Biol.* **209**, 3940-3951.
- Clarke, A. and Johnston, N. M. (1999). Scaling of metabolic rate with body mass and temperature in teleost fish. *J. Anim. Ecol.* **68**, 893-905.
- Coombs, S. and Janssen, J. (1989). Peripheral processing by the lateral line system of the mottled sculpin (*Cottus bairdi*). In *The Mechanosensory Lateral Line*:

- Neurobiology and Evolution* (ed. S. Coombs, P. Göner and H. Münz), pp. 299-319. New York: Springer-Verlag.
- Coombs, S. and Janssen, J.** (1990). Behavioral and neurophysiological assessment of lateral line sensitivity in the mottled sculpin, *Cottus bairdi*. *J. Comp. Physiol. A* **167**, 557-567.
- Correll, N., Sempo, G., Lopez de Meneses, Y., Halloy, J., Deneubourg, J. L. and Martinoli, A.** (2006). SwisTrack: a tracking tool for multi-unit robotic and biological systems. In *Proceedings of the 2006 IEEE/RSJ International Conference on Intelligent Robots and Systems (IROS)*, pp. 2185-2191.
- Coughlin, D. J. and Rome, L. C.** (1996). The roles of pink and red muscle in powering steady swimming in scup, *Stenotomus chrysops*. *Am. Zool.* **36**, 666-677.
- Coughlin, D. J., Zhang, G. and Rome, L. C.** (1996). Contraction dynamics and power production of pink muscle of the scup (*Stenotomus chrysops*). *J. Exp. Biol.* **199**, 2703-2712.
- da Silva, R. and Lange, A. B.** (2011). Evidence of a central pattern generator regulating spermathecal muscle activity in *Locusta migratoria* and its coordination with oviposition. *J. Exp. Biol.* **214**, 757-763.
- Daniel, T. L. and Webb, P. W.** (1987). Physical determinations of locomotion. In *Comparative Physiology: Life in Water and Land* (ed. P. Dejours, L. Bolis, C. R. Taylor and E. R. Weibel), pp. 343-369. New York: Liviana Press.
- Denton, E. J. and Gray, J. A. B.** (1993). Stimulation of the acoustico-lateralis system of clupeid fish by external source and their own movements. *Philos. Trans. R. Soc. Lond. B* **341**, 113-127.
- Dickson, K. A., Donley, J. M., Sepulveda, C. and Bhoopat, L.** (2002). Effects of temperature on sustained swimming performance and swimming kinematics of the chub mackerel *Scomber japonicus*. *J. Exp. Biol.* **205**, 969-980.
- Drucker, E. G.** (1996). The use of gait transition speed in comparative studies of fish locomotion. *Am. Zool.* **36**, 555-566.
- Ellerby, D. J. and Altringham, J. D.** (2001). Spatial variation in fast muscle function of the rainbow trout *Oncorhynchus mykiss* during fast-starts and sprinting. *J. Exp. Biol.* **204**, 2239-2250.
- Farrell, A. P.** (2007). Cardiorespiratory performance during prolonged swim tests with salmonids: a perspective on the temperature effects and potential analytical pitfalls. *Philos. Trans. R. Soc. Lond. B* **362**, 2017-2030.
- Farrell, A. P. and Steffensen, J. F.** (1987). An analysis of the energetic cost of the branchial and cardiac pumps during sustained swimming in trout. *Fish Physiol. Biochem.* **4**, 73-79.
- Fish, F. E.** (1994). Influence of hydrodynamic design and propulsive mode on mammalian swimming energetics. *Aust. J. Zool.* **42**, 79-101.
- Friesen, W. O.** (1994). Reciprocal inhibition: a mechanism underlying oscillatory animal movements. *Neurosci. Biobehav. Rev.* **18**, 547-553.
- Fry, F. E. J.** (1957). The aquatic respiration of fish. In *Physiology of Fishes*, Vol. 1 (ed. M. E. Brown), pp. 1-98. New York: Academic Press.
- Greek-Walker, M. and Pull, G. A.** (1975). A survey of red and white muscle in marine fish. *J. Fish Biol.* **7**, 295-300.
- Hartwell, S. I. and Otto, R. G.** (1991). Critical swimming capacity of the Atlantic silverside, *Menidia menidia* L. *Estuaries* **14**, 218-221.
- Hogan, J. D., Fisher, R. and Nolan, C.** (2007). Critical swimming abilities of late-stage coral reef fish larvae from the Caribbean: a methodological and intra-specific comparison. *Bull. Mar. Sci.* **80**, 219-232.
- Hudson, R. C. L.** (1973). On the function of the white muscles in teleosts at intermediate swimming speeds. *J. Exp. Biol.* **58**, 509-522.
- Iwasaki, T. and Zheng, M.** (2006). Sensory feedback mechanism underlying entrainment of central pattern generator to mechanical resonance. *Biol. Cybern.* **94**, 245-261.
- Jayne, B. C. and Lauder, G. V.** (1995). Red muscle motor patterns during steady swimming in largemouth bass: effects of speed and correlations with axial kinematics. *J. Exp. Biol.* **198**, 1575-1587.
- Jones, D. R.** (1982). Anaerobic exercise in teleost fish. *Can. J. Zool.* **60**, 1131-1134.
- Kolok, A. S.** (1991). Photoperiod alters the critical swimming speed of juvenile largemouth bass, *Micropterus salmoides*, acclimated to cold water. *Copeia* **1991**, 1085-1090.
- Kroese, A. B. A. and Schellart, N. A. M.** (1992). Velocity- and acceleration-sensitive units in the trunk lateral line of the trout. *J. Neurophysiol.* **68**, 2212-2221.
- Liao, J. C.** (2006). The role of the lateral line and vision on body kinematics and hydrodynamic preference of rainbow trout in turbulent flow. *J. Exp. Biol.* **209**, 4077-4090.
- Liao, J. C., Beal, D. N., Lauder, G. V. and Triantafyllou, M. S.** (2003). The Kármán gait: novel body kinematics of rainbow trout swimming in a vortex street. *J. Exp. Biol.* **206**, 1059-1073.
- Lighthill, J.** (1993). Estimates of pressure differences across the head of a swimming clupeid fish. *Philos. Trans. R. Soc. Lond. B* **341**, 129-140.
- Lindsey, C. C.** (1978). Form, function, and locomotory habits in fish. In *Fish Physiology*, Vol. 7 (ed. W. S. Hoar and D. J. Randall), pp. 1-100. New York: Academic Press.
- Lowe, C. G.** (2001). Metabolic rates of juvenile scalloped hammerhead sharks (*Sphyrna lewini*). *Mar. Biol.* **139**, 447-453.
- Lowe, C. G., Holland, K. N. and Wolcott, T. G.** (1998). A new acoustic tailbeat transmitter for fishes. *Fish. Res.* **36**, 275-283.
- McHenry, M. J., Michel, K. B., Stewart, W. and Müller, U. K.** (2010). Hydrodynamic sensing does not facilitate active drag reduction in the golden shiner (*Notemigonus crysoleucas*). *J. Exp. Biol.* **213**, 1309-1319.
- Montgomery, J. C., Coombs, S. and Janssen, J.** (1994). Form and function relationships in lateral line systems: comparative data from six species of Antarctic nototheniid fish. *Brain Behav. Evol.* **44**, 299-306.
- Montgomery, J. C., Coombs, S. and Baker, C. F.** (2001). The mechanosensory lateral line system of the hypogean form of *Astyanax fasciatus*. *Environ. Biol. Fishes* **62**, 87-96.
- Montgomery, J. C., McDonald, F., Baker, C. F., Carton, A. G. and Ling, N.** (2003). Sensory integration in the hydrodynamic world of rainbow trout. *Proc. Biol. Sci.* **270** Suppl. 2, S195-S197.
- Obatake, A. and Heya, H.** (1985). A rapid method to measure dark muscle content in fish. *Bull. Japan. Soc. Sci. Fish.* **51**, 1001-1004.
- Peake, S. J. and Farrell, A. P.** (2006). Fatigue is a behavioural response in respirometer-confined smallmouth bass. *J. Fish Biol.* **68**, 1742-1755.
- Peake, S. J. and McKinley, R. S.** (1998). A re-evaluation of swimming performance in juvenile salmonids relative to downstream migration. *Can. J. Fish. Aquat. Sci.* **55**, 682-687.
- Rome, L. C., Sosnicki, A. and Choi, I.-H.** (1992). The influence of temperature on muscle function in the fast swimming scup. II. The mechanics of red muscle. *J. Exp. Biol.* **163**, 281-295.
- Rowe, D. M., Denton, E. J. and Batty, R. S.** (1993). Head turning in hearing and some other fish. *Philos. Trans. R. Soc. Lond. B* **341**, 141-148.
- Schmidt-Nielsen, K.** (1972). Locomotion: energy cost of swimming, flying, and running. *Science* **177**, 222-228.
- Steffensen, J. F.** (1989). Some errors in respirometry of aquatic breathers: how to avoid and correct for them. *Fish Physiol. Biochem.* **6**, 49-59.
- Steinhausen, M. F., Steffensen, J. F. and Andersen, N. G.** (2005). Tail beat frequency as a predictor of swimming speed and oxygen consumption of saithe (*Pollachius virens*) and whiting (*Merlangius merlangus*) during forced swimming. *Mar. Biol.* **148**, 197-204.
- Tudorache, C., Vianen, P., Blust, R. and De Boeck, G.** (2007). Longer flumes increase critical swimming speeds by increasing burst-glide swimming duration in carp *Cyprinus carpio*, L. *J. Fish Biol.* **71**, 1630-1638.
- Tytell, E. D. and Cohen, A. H.** (2008). Rostral versus caudal differences in mechanical entrainment of the lamprey central pattern generator for locomotion. *J. Neurophysiol.* **99**, 2408-2419.
- Videler, J. J.** (1993). *Fish swimming. Fish and Fisheries Series 10*. London: Chapman & Hall.
- Webb, P. W.** (1975). Hydrodynamics and energetics of fish propulsion. *Bull. Fish. Res. Board Can.* **190**, 1-156.
- Webb, P. W.** (1998). Swimming. In *The Physiology of Fishes* (ed. D. H. Evans), pp. 3-24. New York: CRC Press.
- Webber, D. M., Boutillier, R. G., Kerr, S. R. and Smale, M. J.** (2001). Caudal differential pressure as a predictor of swimming speed of cod (*Gadus morhua*). *J. Exp. Biol.* **204**, 3561-3570.
- Williams, I. V. and Brett, J. R.** (1987). Critical swimming speed of Fraser and Thompson River pink salmon (*Oncorhynchus gorbuscha*). *Can. J. Fish. Aquat. Sci.* **44**, 348-356.
- Xu, G., Arimoto, T. and Inoue, M.** (1993). Red and white muscle activity of the jack mackerel *Trachurus japonicus* during swimming. *Nippon Suisan Gakkai Shi.* **59**, 745-751.